

## THE INFLUENCE OF CO<sup>2+</sup> CONCENTRATION ON THE PROPERTIES OF THE ELECTRODEPOSITED ZINC-COBALT ALLOY COATINGS

MalikaDiafi<sup>1)\*</sup>, Tahraoui Louiza<sup>1)</sup>, Kelthoum Digheche<sup>1)</sup>, Farida Khamouli<sup>1)</sup>

<sup>1)</sup> Physic Laboratory of Thin Films and Applications (LPCMA), University of Biskra, 07000, Algeria

Received: 12.02.2018

Accepted: 08.08.2018

\*Corresponding author: e-mail: diafimalika@gmail.com, Tel.: +213557286468, Physic Laboratory of Thin Films and Applications (LPCMA), University of Biskra, 07000, Algeria

### Abstract

The effects the concentration of cobalt on zinc-cobalt alloys obtained from sulphate baths under continuous current deposition are described. The deposit morphology was analyzed using Scanning Electron Microscopy (SEM) and an X-Ray Diffraction (XRD) was used to determine the preferred crystallographic orientations of the deposits. Protection against corrosion properties studied in a solution of 3 % wt NaCl in the potentiodynamic polarization measurements (Tafel), electrochemical impedance spectroscopy (EIS) to the potential of corrosion free. The parameters that characterize the corrosion behavior can be determined from the plots and Nyquist plots. It has been observed that the Zn-Co alloy is characterized by enhanced the resistance of corrosion compared to the Zn alloys and the addition of Co in the Zn-Co increases the micro-hardness, XRD and SEM results an identify any coatings Zn-Co alloy composition reveals that. zinc - rich ( $\eta$ - phase), cubic Co<sub>5</sub>Zn<sub>21</sub>.

**Keywords:** Cobalt-rich, Zn-Co alloys, electrochemical, deposition, structure, corrosion resistance

### 1 Introduction

Considerable research has been performed to improve the corrosion resistance of metallic surfaces. Zinc coatings are used widely to protect iron and steel substrates against corrosion [1]. Significant research in electrodeposited zinc has been focused on the development of alloy coatings that contain small amounts of other elements, such as Mn, Fe, Co, Sn and Ni, Cr, the most common examples being Zn-Fe [2-3], Zn-Co [2,4-6] and Zn-Ni [2,7-9]. Metals like iron, cobalt and nickel have been incorporated in zinc plating baths to obtain coatings with higher corrosion resistance [1] At high cobalt content (more than 10 wt.%), Zn-Co multilayer coatings have better corrosion resistance than zinc-cobalt single layer coatings as reported by Bahrololoom et al [1].The electrodeposition of Zn-Co alloys with a controlled morphology and composition has been the subject of many studies as a consequence of their observed improved corrosion resistance [1,10-11]. The purpose of our work is the characterization of composites Zn-Co deposits on a mild steel substrate. These deposits are obtained using an acidic sulphate bath, which were introduced from the suspension (CoSO<sub>4</sub>. 6H<sub>2</sub>O) with different concentrations. Technical XRD was used for the structure analysis; SEM was used for morphological analysis. Studies potentiodynamic polarization and electrochemical impedance in a solution of 3 % wt NaCl.

## 2 Experimental

### 2.1 Coating processes

The deposition of Zn–Ni coatings was carried out onto steel substrates under galvanostatic conditions at operating current density of 30 mA/cm<sup>2</sup> and a temperature of 30 °C. The chemical composition of the basic electrolyte of pure Zn coating the plating bath alloys deposition was given in **Table 1** [12,13,14]. Electrodeposits Zn were obtained by varying the concentration of Co in the bath (0, 5 and 0.1, 0.15 M).

### 2.2 Coating characterization

XRD characterization of samples was carried out with a D8 Advance-Brucker using a Cu K $\alpha$  radiation with the wavelength  $\lambda = 0.1540$  nm and 0.02° step.

Scherrer's formula is used for the determination of the Crystallite sizes of the coatings from the X-ray peak broadening of the (101) diffraction peak [15,16]:

$$D = \frac{0,9\lambda}{\beta \cos\theta} \quad (1)$$

Where D is the grain size,  $\lambda$  is the X-ray wavelength ( $\lambda = 1.540$  nm),  $\beta$  is the corrected peak full width at half maximum intensity (FWHM), and  $\theta$  is Bragg angle position of peak.

The surface morphology of different Zn–Co deposits was observed by a JEOL JSM 5800 scanning electron microscope (SEM). Micro hardness of coatings was measured using a load of 100 g with a holding time of 15 s by using a Vickers hardness tester (HV) of deposits were performed in the surface by using a Wolpert Wilson Instruments (model 402UD) [12].

**Table 1** Basic solution and conditions for alloy coatings

Basic solution	Concentration(g·l <sup>-1</sup> )	Plating parameters
ZnSO <sub>4</sub> ·7H <sub>2</sub> O	57.5	30°C and pH=3-4,5 constant current densities at 30 mA/cm <sup>2</sup> for 60 s
H <sub>3</sub> BO <sub>3</sub>	9.3	
Na <sub>2</sub> SO <sub>4</sub>	56.8	
Na <sub>3</sub> C <sub>6</sub> H <sub>5</sub> O <sub>7</sub>	56.8	

### 2.3 Electrochemical measurements

The corrosion behavior and the protection performance of Zn and Zn–Co alloy coatings were studied by using of electrochemical impedance spectroscopy (EIS) and electrochemical Tafel extrapolation in 3 % wt NaCl solution. The tests were performed using a potentiostat galvanostat (a Volta Lab 40 model), the electrode of work was a coated sample, the counter electrode was platinum with a surface of 1 cm<sup>2</sup> and the Hg/HgO/ 1 M KOH is used as reference electrode. Whereas the impedance data were obtained at the open-circuit potential and the measurements were carried out over a frequency range of 100 KHz–10 MHz using an amplitude of sinusoidal voltage (10 mV). The potentiodynamic polarization was carried out at a scan rate of 50 mV/s and the scanning potential ranged from –1500mV to +1500mV of open circuit potential. The corrosion current density and corrosion potential were determined based on Tafel's extrapolation

## 3 Results and discussions

### 3.1 X-ray diffraction

**Fig. 1** Shows the X-ray diffraction patterns obtained for several Zn and Zn-Co alloy deposits. In the absence of cobalt, the peaks associated with the characteristic crystallographic planes for zinc were observed, The diffraction lines corresponding to zinc-rich  $\eta$ - phase, cubic  $\text{Co}_5\text{Zn}_{21}$  (101) and the peak associated with plane (002) having the highest intensity, the presence of cobalt (0.05, 0.1 and 0,15 M) in the alloy coatings slightly decreases the intensities of the diffracted planes as compared with those of the pure zinc. With an increase in cobalt content in Zn–Co alloy deposits, the intensity of peaks for planes (002), (100), and (101) decreases further. This decrease of intensity is also observed in other peaks related to phase of zinc-rich; The Zn–Co alloy coatings have the same structure as zinc. single phase structure ( $\eta$ -phase , cubic  $\text{Co}_5\text{Zn}_{21}$ ) which is a solid solution of cobalt in zinc [17,18].

**Table 2** shows the relationship between cobalt content and grain size of Zn–Co alloy coatings. Crystallite sizes of the coatings were calculated from the X-ray peak broadening of the (101) diffraction peak using Scherrer's formula. Zn pure alloy, deposited in Basic solution, exhibited a crystallite size of 72 nm, whereas the crystallite size of Zn alloy coating deposited in electrolyte Basic solution+0,15 M  $\text{Co}^{2+}$  decreased to 51,08 nm. where the grain sizes diminish in the presence of cobalt ions, This finer structure explained probably the higher hardness of this deposit mentioned previously [19].

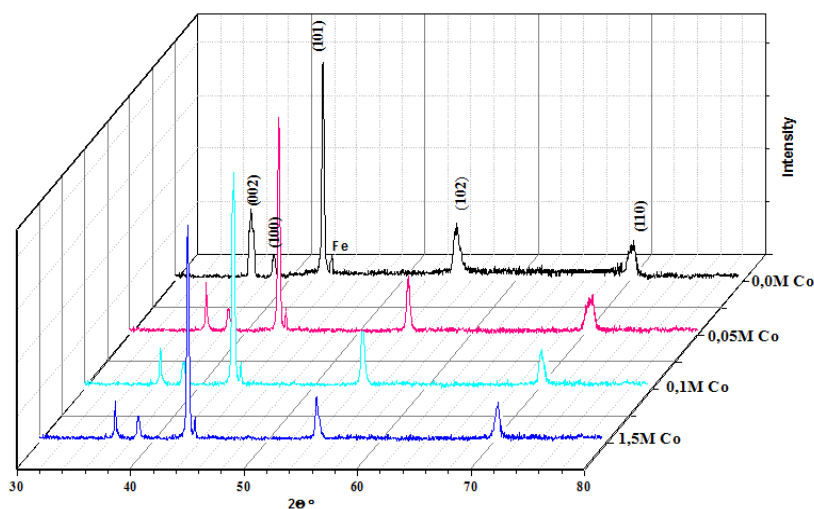


**Fig. 1** X-ray diffraction patterns for Zn and alloy electrodeposits obtained at 30 mA/cm<sup>2</sup>, T = 30 °C, and pH 3-4, 5 for 60 s. Bath cobalt concentrations: 0.0 M , 0.05 M , 0.1 M , 0.15 M

**Table 2** Values of the FWHM and crystallite size obtained from the strongest diffraction line of the metallic phases

Electrolyte	FWHM	Crystal size/nm
Basic solution	0.11	72
Basic solution+ 0.05 M Cobalt	0.12	68.1
Basic solution+ 0.1 M Cobalt	0,23	59,77
Basic solution+ 0.15 M Cobalt	0,28	51,08

### 3.2 Effect of Cobalt content of the bath on coatings micro hardness

The variation of microhardness vs cobalt content in the deposited Zn–Co alloy coatings is shown in **Fig. 2** and **Table 3**. This figure indicates that the micro hardness of Zn–Co alloy coatings increases with increasing cobalt content. This is because that the hardness of Co is greater than Zn, The hardness increased from 225 Hv for Zn, alloy to 250 and 310 Hv for 0.05 and 0.15M Co alloy coating respectively, Hardness values enhance with Co content, it can be correlated to the (i) formation of solid solution, (ii) formation of two phase structure, (iii) grain size effects [19-22].

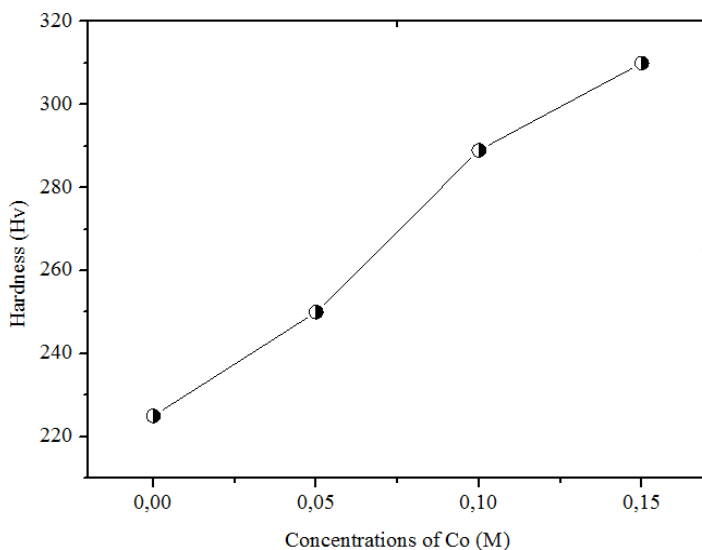


**Fig. 2** The effect of cobalt contents in the composite coatings on the hardness of deposits. Zn–Co alloy coating

**Table 3** Values of micro-hardness Vickers hardness (HV) registered different electro deposition

Coating	microhardness (HV)
Basic solution	225
Basic solution + 0.05 M Cobalt	250
Basic solution + 0.1 M Cobalt	289
Basic solution + 0.15 M Cobalt	310

### 3.3 Surface morphology

Scanning electron micrographs of the electrodeposits obtained from the acidic sulphate Zn and Zn–Co baths are shown in **Fig. 3**. The surface of Pure Zn alloy coating (**Fig. 3a**) is uniform, homogenous and consists of irregular crystals particles, have a clear grey colour, the Zn–Co alloy (**Fig. 3b, 3c** and **3d**) appear sufficiently well distributed, compact and continuous, homogeneity, having a clear brown colour, It is clear that the grains size is decreased with the increase of cobalt content in the Zn-Co deposits, The presence of cobalt modifies the growth of the zinc nuclei, leading to fine-grained deposits. Consequently, the compactness, adherence and hardness increase with elevation of the Cobalt content [1,15,20, 21,23].

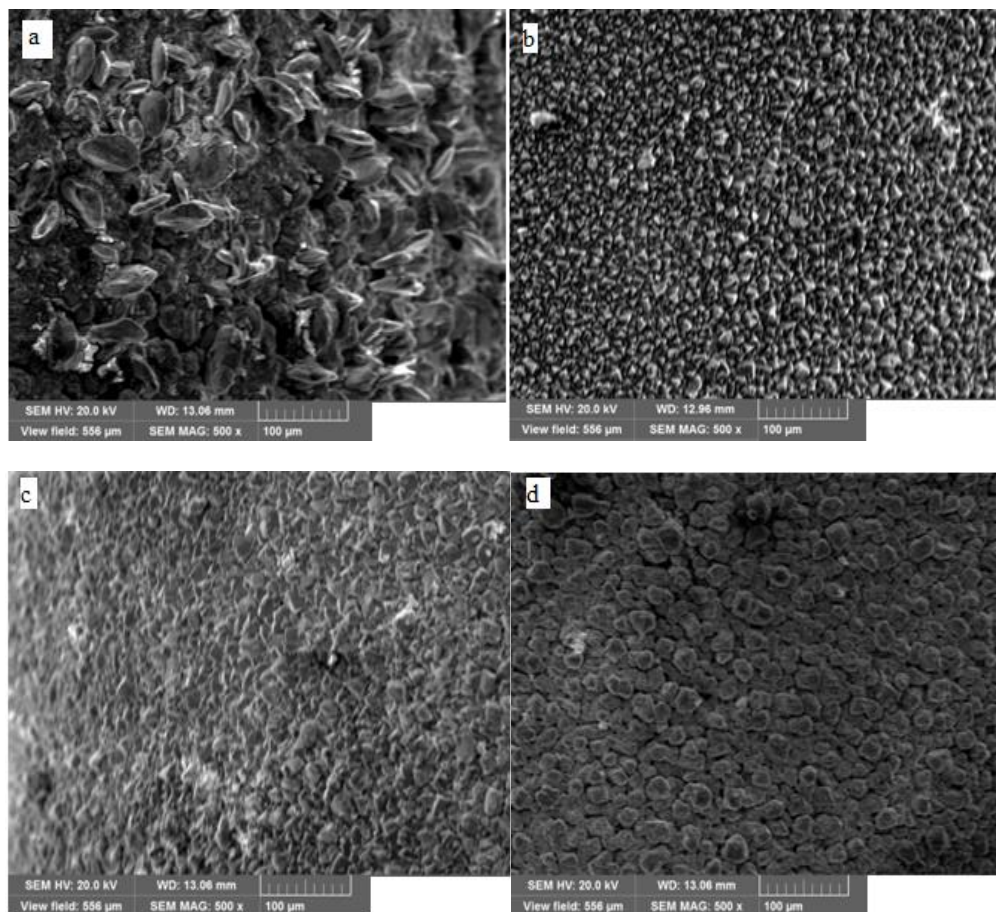


**Fig. 3** Surface morphology of :**(a)** Zn alloy coatings ,**(b)** Zn–Co (0,05 M Co) , **(c)** Zn– Co (0,1M Co) , **(d)** Zn– Co(0,15M Co) Composite coatings deposited at 30 mA/cm<sup>2</sup>, T = 30 °C, and pH 3-4,5 for 60 s

### 3.4 Corrosion studies

#### 3.4.1 Cyclic Voltammetry Study

**Fig. 4** shows cyclic voltammograms of the specimen exposed to electrolyte containing ZnSO<sub>4</sub> and different concentrations of cobalt from 0.05 to 0.15 M with potential scan rate of 50 mV s<sup>-1</sup> at room temperature, the anodic part of the cyclic voltammetry consists of first anodic peaks. The height of the first dissolution anodic, peak decreases with increasing cobalt concentration in the plating bath. It is observed that the reduction potential of Zn–Co alloy does not change considerably, when concentration in electrolyte increases. It is also seen that in the anodic part of cyclic voltammetry, when cobalt concentration increases from 0.05 to 0.15 M, the anodic peak potential moves gradually toward more positive values, and the anodic peak current reduces. These variations show that if the Cobalt concentration in electrolyte increases the amount of Zinc in the alloy decreases and the formation of Cobalt in the deposited alloy increases. Besides, by increasing of cobalt concentration in the electrolyte from 0.05 to 0.15 M, only one anodic peak is observed, this indicates of solid solution formation of cobalt in zinc [18].

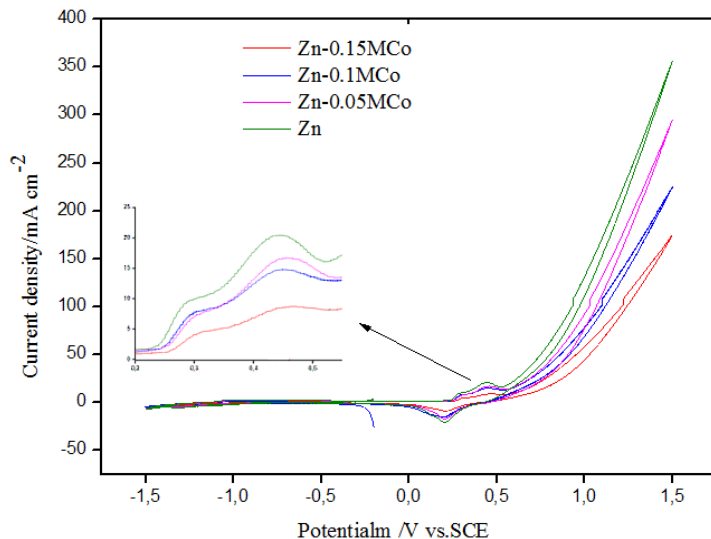


**Fig. 4** Cyclic voltammetric study for deposition Zn–Co alloy in Co ions at different molar concentrations at 25°C and scan rate of 50 mV s<sup>-1</sup>

**Fig. 5** shows cyclic voltammograms obtained from the electrolyte containing 0.1 M CoSO<sub>4</sub> at five different scan rates of 5, 10 and 20, 50, 100 mV s<sup>-1</sup>. It is observed that when scan rate increases from 5 to 100 mV s<sup>-1</sup>, cathodic peak potential moves toward more negative values, and anodic peak potential moves toward more positive values. Therefore, with the increase of scan rate, the distance between anodic and cathodic peaks increases. This increase is related to the loss of ohmic drop [18]. **Fig 5** also indicates that the reduction–oxidation (redox) reactions of in Zn–Co alloy are quasi-reversible, because the ratio of cathodic to anodic peak current is almost close to one

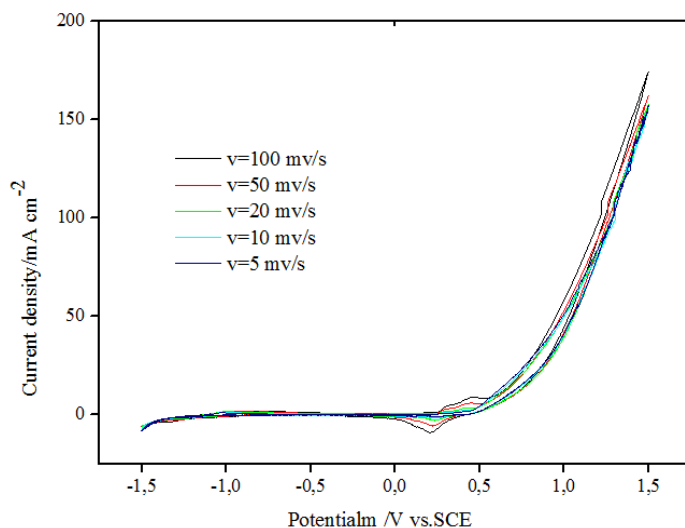


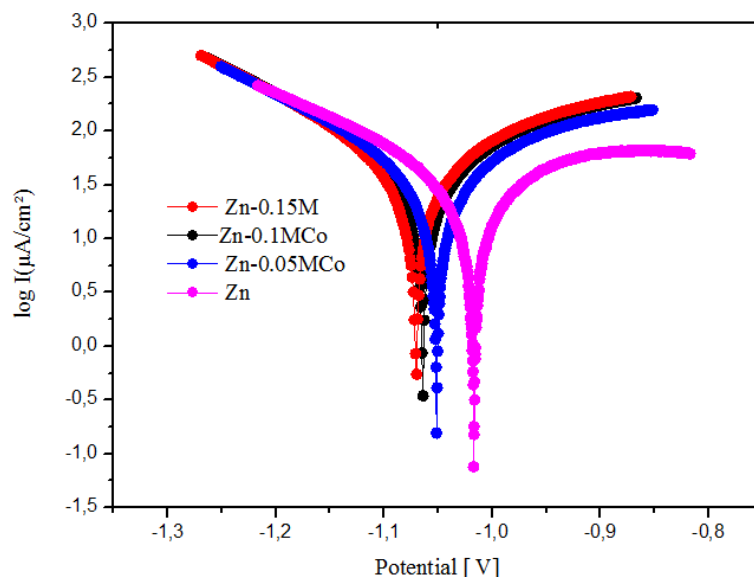
**Fig. 5** Cyclic voltammograms for the electrodeposition on steel in electrolyte containing: 0.1 M CoSO<sub>4</sub>, at room temperature with different scan rates: 5, 10 and 20 , 50, 100 mV s<sup>-1</sup>

**Table 4** The electrochemical parameters ( $E_{corr}$ ,  $I_{corr}$ ,  $\beta_a$ ,  $\beta_c$ ) of the coatings samples in a 3 % wt NaCl solution

Coating	$E_{corr}$ (mV)	$I_{corr}$ (mA/cm <sup>2</sup> )	$\beta_a$ (mV)	$\beta_c$ (mV)
Basic solution	-1,0297	0,0749	49	-220 ,3
Basic solution + 0.05 M Cobalt	-1,0515	0,1562	133,1	-261,2
Basic solution + 0.1 M Cobalt	-1,063	0,346	147,2	-294 ,8
Basic solution + 0.15 M Cobalt	-1,1515	0,549	144 ,2	-296 ,7

### 3.4.1 Potentiodynamic polarization studies

**Fig. 6** illustrates the polarization curves obtained from potentiodynamic polarization tests in 3 wt% NaCl solution for Zn–Co alloy coatings. The corrosion potential ( $E_{corr}$ ) and corrosion current density ( $I_{corr}$ ) calculated from the intersection of the cathodic and anodic Tafel slopes in the range of  $\pm 50$  mV of the open-circuit potential ( $E_{ocp}$ ). Values were determined from this figure and cited in in **Table 4**.

**Fig. 6** Polarizing curves obtained for the alloy coatings in a 3 wt % NaCl solution at different concentrations of Co

Deposited alloys from sulphate bath with lower Cobalt concentration (0.05) have slightly higher  $I_{corr}$  values as compared with deposited alloys from sulphate bath with higher Cobalt concentration (0.15 M) (**Table 4**), which is probably can be the consequence of smaller Co content in the deposit, since higher Cobalt content in the plating bath results the higher Cobalt amount in the deposit [17]. increasing the Co concentration in the plating bath increases the corrosion resistance of the deposit. The derived polarization resistance ( $R_p$ ) values indicated that the Zn–Co alloy exhibits much higher corrosion resistance than pure zinc ( $R_p$ , Zn = 80 ,46 $\Omega$  cm<sup>2</sup> vs  $R_p$ , Zn-0.15 MCo = 93,45 $\Omega$  cm<sup>2</sup>) [20, 24].

### 3.4.3 Electrochemical impedance spectroscopy (EIS) studies

EIS studies have been performed in 3 wt. % NaCl solution to evaluate corrosion resistance behavior of the samples. As seen in **Fig. 7**, Nyquist responses of all samples are in depressed semicircle (unfinished) shape. The diameter of this semicircle reflects the corrosion resistance of the related sample. As can be seen, the semicircle diameter of the sample obtained at 0.15 M Co is the biggest and the semicircle diameter of sample obtained at Zn is the lowest one (The increase in the size of the capacitive loop with the addition of Co). This can be attributed to the charge transfer resistance control of the corrosion reactions of the samples because of the domination Zn-rich phases in the coatings. The EIS plots shown in **Fig. 7** are analyzed using one time-constant electrochemical equivalent circuit (EEC) model and fitted through EC-Lab program. The represented elements shown in the circuit are  $R_s$  (solution resistance),  $R_t$  (charge transfer resistance of the electrode reactions) and CPE (Constant Phase Element), representing the double layer capacitance between the solution and the alloy coating. Extracted fitted data from the equivalent circuit is shown in **Table 5**.

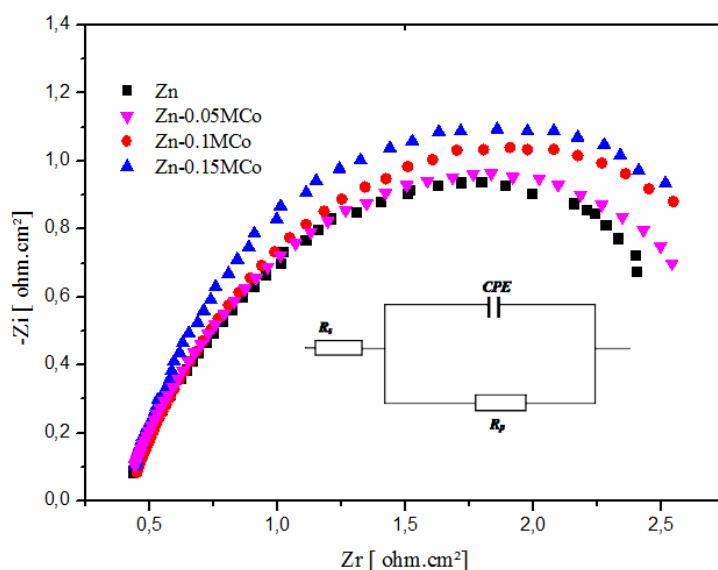


**Fig. 7** The Nyquist plots obtained for Zn–Co alloy coatings electrodeposited at different concentrations of Co

**Table 5** Extracted fitted data from the equivalent circuit of Zn–Co alloy coatings in a 3 % wt NaCl solution

Coating	$R_p$ ( $\Omega \cdot \text{cm}^2$ )	$R_s$ ( $\Omega \cdot \text{cm}^2$ )	CPE ( $\mu\text{F}/\text{cm}^2$ )
Basic solution	80,46	7.964	0.965
Basic solution + 0.05 M Cobalt	83,20	10.5	0.911
Basic solution + 0.1 M Cobalt	91,39	13.14	0.8208
Basic solution + 0.15 M Cobalt	93,45	15.23	0.541

#### 4 Conclusion

The following conclusions were drawn:

- XRD spectres illustrate the phase structure of composites coating was single zinc-rich ( $\eta$ - phase), cubic  $\text{Co}_5\text{Zn}_{21}$  and incorporation of cobalt in the Zn-Co alloy coating decrease the grain size.
- From the SEM images of the composites coating morphologies the grains size decreases with the increase of cobalt content in the Zn-Co deposits.
- The test of the micro-hardness on the various electro deposited coatings has a maximum value (0.15 M) Co, because the increase of the Co concentration in the plating bath increases of micro-hardness.
- Also the surface morphology of the deposits was improved with increasing Co concentration, gives a more uniform surface morphology and more compact deposits.
- The height of the first dissolution anodic, peak decreases with increasing cobalt concentration in the plating bath.
- The study by the method from potentiodynamic polarization curves showed that the values of the corrosion potential ( $E_{\text{corr}}$ ) decreases, the corrosion current density ( $I_{\text{corr}}$ ) and the polarization resistance ( $R_p$ ) increases with increasing the concentration of Cobalt in the electrolyte bath.
- EIS analysis performed on the developed coatings that have increased resistors  $R_s$ . The increase in the size of the capacitive loop with the addition of Cobalt.

#### References

- [1] J.L. Ortiz-Aparicio, Y. Measa, G. Trejo, R. Ortega, T.W. Chapman, E. Chainet, P. Ozil: *Electrochimica Acta*, Vol. 52, No. 14, 2007, p. 4742–4751, DOI: 10.1016/j.electacta.2007.01.010
- [2] A.B. Velichenko, J. Portillo, X. Alcobe, M. Sarret, C. Muller: *Electrochimica Acta*, Vol. 46, 2000, No. 2-3, p. 407–414, DOI: 10.1016/S0013-4686(00)00599-5
- [3] G.D. Wilcox, R.D. Gabe: *Corrosion Science*, Vol. 35, No. 5-8, 1993, p. 1251- 1258. DOI: 10.1016 / 00 10-938X(93)90345-H
- [4] K. Higashi, H. Fukushima, T. Urokawa, T. Adanya, K. Matsudo: *Journal of Electrochemical Socience*, Vol. 128, No. 10, 1981, p. 2081-2085, DOI: 10.1149/1.2127194
- [5] E. Gomez, E. Valles : *Journal of Electroanalytical Chemistry*, Vol. 421, No. 1-2, 1997, p. 157-163, DOI:10.1016/S0022-0728(96)04835-8
- [6] R. Fratesi, G. Roventi, G. Giuliani, C.R. Tomachuk: *Journal of Applied. Electrochemistry*, Vol. 27, No. 9, 1997, p. 1088–1094, DOI:10.1023/A:1018494828198
- [7] L. Felloni, R. Fratesi, E. Quadrini, G. Roventi : *Journal of Applied. Electrochemistry*, Vol. 22, No. 7, 1992, p. 657–662, DOI:10.1007/BF01092615
- [8] G. Barcelo, J. Garcı, M. Sarret, C. Muller, J. Pregonas: *Journal of Applied. Electrochemistry* , Vol. 24, No. 12, 1994, p. 1249–1255, DOI:10.1007/BF00249889
- [9] M. Mouanga , L. Ricq, P. Berçot : *Surface and Coatings Technology*, Vol. 202, No. 9, 2008, p. 1645–1651, DOI:10.1016/j.surfcoat.2007.07.023
- [10] P.Y. Chen, I.W. Sun : *Electrochim. Acta*, Vol. 46, No. 8, 2001, p. 1169 –1177, DOI: 10.1016/S0013-4686(00)00703-9
- [11] C.R. Tomachuk, C.M.A. Freire, M. Ballester, R. Fratesi, G. Roventi : *Surface and Coatings Technology*, Vol. 122 , No. 1, 1999, p. 6-9, DOI: 10.1016/S0257-8972(99)00400-4

- [12] M. Diafi, S. Benramache, E. Guettaf Temam, A. Mohamed Lakhdar, B. Gasmi: Acta Metallurgica Slovaca, Vol. 22, 2016, No. 3, p. 171-180, DOI:10.12776/ams.v22i3.706
- [13] O. Hammami, L. Dhouibi, P. Berçot, E. Rezzazi: Surface & Coatings Technology, Vol. 219, 2013, p. 119–125, DOI:10.1016/j.surfcoat.2013.01.014
- [14] M. Diafi, N. Belhamra, H. Ben Temam, B. Gasmi, S. Benramache: Acta Metallurgica Slovaca, Vol. 21, No. 3, 2015, p. 226-235, DOI: 10.12776/ams.v21i3.472
- [15] M.S. Chandrasekar, S. Shanmugasigamani, M. Pushpavanam: Materials Chemistry and Physics, Vol. 115, No. 2-3, 2009, p. 603–611, DOI:10.1016/j.matchemphys.2009.01.020
- [16] J. L. Ortiz-Aparicio, Y. Meas, G. Trejo, R. Ortega, T. W. Chapman, E. Chainet, P. Ozil: Journal of Applied. Electrochemistry, Vol. 41, 2011, p. 669–679, DOI: 10.1007/s10800-011-0279-y
- [17] J. B. Bajat, V. B. Miskovic-Stankovic, M. D. Maksimovic, D. M. Drazic & S. Zec, Electrochim Acta, Vol. 47, 2002, p. 4101-4112
- [18] M. Heydari Gharahcheshmeh, M. Heydarzadeh Sohi: Journal of Applied. Electrochemistry, Vol. 40, No. 8, 2010, p. 1563–1570, DOI: 10.1007/s10800-010-0142-6
- [19] B. Bakhit, A. Akbari: Journal of Coatings Technology and Research, Vol. 10, 2013, No. 2, p. 285–295, DOI:10.1007/s11998-012-9437-3
- [20] M. Diafi, K. Degheche, H. Ben Temam: Journal of Fundamental and Applied Sciences, Vol. 9, No. 1, 2017, p. 89-101, DOI: 10.4314/jfas.v9i1.7
- [21] A.M. Alfantazi, U. Erb: Materials Science and Engineering A, Vol. 212, 1996, No. 1, p. 123–129, DOI:10.1016/0921-5093(96)10187-8
- [22] L. S. Tsybul'skaya, T. V. Gaevsкая, T. V. Byk, G. N. Klavsut: Russian Journal of Applied Chemistry, Vol. 74, 2001, No. 10, p. 1678-1682
- [23] M. Mouanga, L. Ricq, P. Berçot: Journal of Applied, Electrochemistry, Vol. 38, 2008, p. 231–238, DOI: 10.1007/s10800-007-9430-1
- [24] S. Lichušina, A. Chodosovskaja, A. Sudavičius, R. Juškėnas, D. Bučinskienė, A. Selskis, E. Juzeliūnas: Chemija, Vol. 19, 2008, No. 1, p. 25–31

### Acknowledgments

*I would like to thank "Responsible Of Laboratory Of Thin Films And Applications" for their assistance in the preparation of this work.*